Articles

Calcium-Dependent Binding of Recoverin to Membranes Monitored by Surface Plasmon Resonance Spectroscopy in Real Time†

Christian Lange and Karl-Wilhelm Koch*

Institut für Biologische Informationsverarbeitung, Forschungszentrum Jülich, Postfach 1913, D-52425 Jülich, Germany

Received April 22, 1997; Revised Manuscript Received July 14, 1997⊗

ABSTRACT: Recoverin is an N-myristoylated Ca^{2+}-binding protein that serves as a Ca^{2+}-sensor in visual transduction. We studied the dynamics of its Ca^{2+}-dependent membrane association which depends on the myristoyl modification (Ca^{2+}−myristoyl switch) by surface plasmon resonance spectroscopy. Either recoverin or phospholipid vesicles were immobilized on a sensor chip surface, and the respective binding partner was supplied in the mobile phase. Binding of recoverin to artificial liposomes or rod outer segment membranes was strictly dependent on Ca^{2+} and the myristoyl group. The Ca^{2+}−myristoyl switch was half-maximal between 4.0 and 7.7 μM Ca^{2+}, depending on whether recoverin or liposomes were in the mobile phase. At saturating [Ca^{2+}], the dissociation constant (K_D) of recoverin for phospholipid liposomes was approximately 150 μM. The association and dissociation of recoverin to membranes was fast and biphasic (fast and slow components) with time constants on the order of 0.1 s^{-1} and 0.01 s^{-1}, respectively. Dissociation of the recoverin−membrane complex was 3-fold faster at low than at high free [Ca^{2+}]. We discuss the analogy between the liposome−sensor chip and the disk surface and conclude that a minor fraction of the total recoverin in a rod outer segment is associated with membranes at resting dark levels of free [Ca^{2+}].

Myristoyl switches of proteins have attained wide interest due to their increasingly recognized importance in signal transduction pathways (*1, 2*). Many proteins involved in signal transduction pathways are N-terminally acylated by myristic acid or related fatty acids (i.e., C12:0; C14:1; C14:2). In some cases, this modification has been shown to be necessary for association of a protein to cellular membranes. If additional cofactors control the membrane binding, the myristoyl moiety constitutes a part of a molecular switch, the so-called myristoyl switch. For example, GTP controls the reversible association of the ADP-ribosylation factor to membranes by a GTP−myristoyl switch (*3, 4*), whereas phosphorylation of myristoylated alanine-rich C kinase substrate (MARCKS) relocates the protein from the membrane to the cytosol (*5*). Ca^{2+}−myristoyl switches have been described for Ca^{2+}-binding proteins like recoverin, neurocalcin, and hippocalcin, that function as Ca^{2+}-sensors and partition into the membrane when their hydrophobic anchor is exposed at high free Ca^{2+} concentrations ([Ca^{2+}])[1] (*6*−*10*). The structural basis of the Ca^{2+}−myristoyl switch has been studied for recoverin by NMR spectroscopy in aequeous solution. In its Ca^{2+}-free form, the myristoyl group is buried inside a hydrophobic pocket of the protein and makes contact with aromatic residues. When Ca^{2+} is bound to recoverin, the acyl group is exposed to the solvent (*11*−*16*).

Bovine recoverin and the frog homologue *S*-modulin both suppress rhodopsin phosphorylation by inhibition of rhodopsin kinase at high [Ca^{2+}] and thereby participate in feedback mechanisms that underlie vertebrate photoreceptor light adaptation (*17*−*21*). Although N-myristoylation of recoverin is not necessary for the inhibitory effect on rhodopsin kinase (*22, 23*), three consequences of acylation of recoverin have been reported: (i) Acylation induces cooperativity of Ca^{2+} binding and thereby might explain the cooperativity of the Ca^{2+}-dependent inhibition of rhodopsin kinase (*23, 24*). (ii) It shifts the EC_{50} value for Ca^{2+} to higher concentrations (*23*). (iii) Acylation stabilizes the complex of Ca^{2+}-recoverin/rhodopsin kinase by promoting the membrane association of recoverin (*25*).

To further our understanding of the molecular mechanism of the Ca^{2+}−myristoyl switch of recoverin, we investigated the dynamics of its membrane association by surface plasmon resonance spectroscopy (*26*−*28*). The experiments were aimed at answering the following questions:

What are the kinetic properties of the binding of myristoylated recoverin to phospholipid vesicles and to native rod outer segment membranes? What are the affinities for the recoverin/phospholipid interaction? What is the range of [Ca^{2+}] at which the association occurs?

† Supported by a grant from the Deutsche Forschungsgemeinschaft (Ko948/5-1).

* Correspondence should be addressed to this author at the Institut für Biologische Informationsverarbeitung, Forschungszentrum Jülich, Postfach 1913, D-52425 Jülich, Germany. Phone: 49-2461-61-3255. Fax: 49-2461-614216. E-mail: koch@ibi.ibi.kfa-juelich.de.

⊗ Abstract published in *Advance ACS Abstracts,* September 15, 1997.

[1] Abbreviations: [Ca^{2+}], concentration of Ca^{2+}; SPR, surface plasmon resonance; biotin-LC-DPPE, *N*-[6-(biotinoylamino)hexanoyl]dipalmitoyl-L-α-phosphatidylethanolamine; PMSF, phenylmethanesulfonyl fluoride; NHS, *N*-hydroxysuccinimide; EDC, *N*-ethyl-*N*′-[(dimethylamino)propyl]carbodiimide; PDEA, 2-(2-pyridinyldithio)-ethaneamine hydrochloride; RU, resonance units; R_{eq}, resonance units at equilibrium; dibromo-BAPTA, 1,2-bis[2-bis(*o*-amino-5-bromophenoxy)ethane]-*N*,*N*,*N*′,*N*′-teraacetic acid.

S0006-2960(97)00938-0 CCC: $14.00

MATERIALS AND METHODS

Materials. Bovine retinae were prepared freshly from bovine eyes obtained from the local slaughterhouse and stored frozen at −80 °C until used. *N*-[6-(Biotinoylamino)-hexanoyl]dipalmitoyl-L-α-phosphatidylethanolamine (biotin-LC-DPPE) was from Pierce. Bovine brain phosphatidylcholine, bovine brain phosphatidylserine, and egg yolk phosphatidylethanolamine were from Sigma and 98% pure. Polycarbonate filter membranes (type GTTP) were from Millipore. All other reagents and buffers were at least analytical grade.

Purification of Proteins. Native recoverin (calculated molecular mass = 23.3 kDa) was purified from bovine ROS (*29*) or from a bovine retina extract (*30*) using hydrophobic interaction and anion exchange chromatography. Briefly, 50 frozen bovine retinae were thawed in 60 mL of buffer A (100 mM NaCl, 20 mM Tris-HCl, pH 8.0, 1 mM DTT, and 0.1 mM PMSF) plus 1 mM EDTA and homogenized with a glass Teflon homogenizer. The suspension was centrifuged at 260 000*g* for 20 min. The supernatant was adjusted to 3 mM $CaCl_2$ and applied to a phenyl-Sepharose column (15 mL) equilibrated in buffer A containing 2 mM $CaCl_2$. Fractions containing recoverin were eluted with buffer A plus 1 mM EGTA and adjusted to the starting buffer of the MonoQ anion exchange chromatography (25 mM NaCl, 20 mM Tris-HCl, pH 8.0) by dilution with 20 mM Tris, pH 8.0. Recoverin was eluted on a gradient of NaCl. A recoverin cDNA clone (kindly provided by Dr. W. Bönigk, IBI-1, Forschungszentrum Jülich) containing the whole coding region of recoverin was subcloned into a pGEX-2T expression vector (Pharmacia), and recombinant recoverin was heterologously expressed as a glutathione *S*-transferase fusion protein in *E. coli* strain XL1Blue. The expressed protein was purified from bacterial cell lysate by glutathione affinity chromatography, thrombin cleavage, and anion exchange chromatography as previously described for GCAP-1 (*31*). Protein concentration was determined according to Bradford with BSA as standard. For storage, proteins were dialyzed against 50 mM $(NH_4)HCO_3$ and lyophilized.

Immobilization of Proteins. Biospecific interactions including all immobilization protocols were performed and monitored by surface plasmon resonance (SPR) using the BIAcore technology (Pharmacia). The carboxylated dextran matrix of BIAcore sensor chips (CM5, Pharmacia) was activated by 10 μL of 50 mM *N*-hydroxysuccinimide (NHS) and 200 mM *N*-ethyl-*N*′-[(dimethylamino)propyl]carbodiimide (EDC) at a flow rate of 5 μL/min. Recoverin was coupled via its free amino groups at a flow rate of 5 μL/min for 7 min (40 μg/mL recoverin in 10 mM sodium acetate, pH 3.5). Activated dextran groups were deactivated by a pulse of 1 M ethanolamine (7 min). Alternatively, recoverin was immobilized by the thiol ligand method. The dextran matrix was activated by NHS/EDC as above and subsequently modified by injection of 20 μL of 80 mM 2-(2-pyridinyldithio)ethaneamine hydrochloride (PDEA) in 0.1 M sodium borate, pH 8.5. Recoverin (20 μg/mL) was immobilized by thiol disulfide exchange at a flow rate of 5 μL/min for 7 min in 0.1 M sodium citrate, pH 3.0. Deactivation was performed by 15 μL of 50 mM cysteine in 1 M NaCl/0.1 M sodium formate, pH 4.3. Changes in resonance units after completion of the immobilization step indicated a surface concentration of recoverin of 1.7−2.9 ng/mm^2.

Preparation of Liposomes and ROS Vesicles. A mixture of 4 mg of lipids [40% w/w PE, 40% w/w PC, 15% w/w PS, and 5% w/w cholesterol, corresponding to the lipid composition in bovine ROS membranes (*32*)] in $CHCl_3$ was dried down by vacuum in a speed vac concentrator, and the resulting phospholipid film was dried over silica gel in a desiccator overnight. The sample was resuspended in degassed buffer (20 mM Hepes, pH 7.5, 150 mM KCl, and 2 mM $MgCl_2$) under argon and sonified for 3 × 5 s (Branson B12; cup; 100 W). Large unilamellar vesicles (liposomes) were produced using the extrusion technique. The suspension was soaked for 2 h and extruded 5 times through a polycarbonate filter (pore diameter = 200 nm).

Biotinylated liposomes from ROS were prepared as follows. Five hundred microliters of ROS (5−6 mg of rhodopsin) was diluted with 2 mL of 10 mM Hepes, pH 7.5, and centrifuged for 15 min at 90 000*g*. The pellet was resuspended in the same buffer, and the centrifugation was repeated. This was followed by two more washing steps with the same buffer containing 10 mM EDTA. The membranes were washed with 10 mM Hepes, pH 7.5, 150 mM KCl, and 2 mM $MgCl_2$ and resuspended in 1 mL of the same buffer. The suspension was then transferred into a vial in which the appropriate amount (1/100 by weight, referring to rhodopsin) of *N*-[6-(biotinoylamino)hexanoyl]dipalmitoyl-L-α-phosphatidylethanolamine (biotin-LC-DPPE) had been dried down under vacuum. To suspend the biotinylated phospholipids, the suspension was sonicated briefly (2 × 5 s). Membranes were labeled with biotin-LC-DPPE by repeated freezing (3×) in liquid nitrogen and thawing to room temperature. Finally, the membranes were extruded successively through polycarbonate filters with pore widths of 1000, 400, and 200 nm to yield ROS liposomes. Phospholipid content was determined by measuring inorganic phosphate (*33*).

Immobilization of Liposomes. Liposomes used as immobilized ligands in SPR experiments were labeled by the addition of 0.1% (w/w) biotin-LC-DPPE. Biotinylated liposomes or ROS vesicles were immobilized on sensor chips containing streptavidin (SA, Pharmacia) via biotin−streptavidin coupling (*34*). A suspension of 150 μL (1−2 mM P_i) was injected at a flow rate of 5 μL/min in 10 mM Hepes, pH 7.5, 150 mM KCl, and 2 mM $MgCl_2$.

Surface Plasmon Resonance Measurements and Data Evaluation. Binding of recoverin to liposomes and ROS membranes was monitored by surface plasmon resonance (BIAcore, Pharmacia). The immobilized binding partner is always termed the *ligand* and the interaction partner in the running buffer the *analyte* (*26*). The running buffer contained 10 mM Hepes, pH 7.5, 150 mM KCl, $MgCl_2$, and Ca^{2+} buffers as indicated (see below). Interaction of recoverin with immobilized liposomes or ROS vesicles was tested by applying up to 2300 μg/mL protein in running buffer at different $[Ca^{2+}]$ and 20 mM $MgCl_2$; the pH was 7.1. Interaction of liposomes with immobilized recoverin was tested by applying up to 1 mM phospholipid in the running buffer with $[Ca^{2+}]$ and $MgCl_2$ as indicated. All measurements were performed at 25 °C. The flow rate was always 10 μL/min.

Binding and dissociation of the analyte were monitored by a change in refractive index close to the surface of the

thin gold film of the sensor chip. Changes in refractive index are correlated to changes in resonance units (RU). Any time-dependent change in refractive index is recorded in real time to yield a sensorgram. The data sampling rate was 1 Hz. Resonance units at equilibrium, R_{eq}, when the net binding rate is zero, were determined from an extrapolation of a dRU/dt vs RU plot (*28*). In each case, for the reaction approaching equilibrium, a linear part of the dRU/dt vs RU plot comprising at least 30 data points (30 s) was identified and extrapolated to dRU/dt = 0. Sensorgrams recorded with liposomes immobilized on a streptavidin-coated sensor chip surface were corrected for nonspecific binding of recoverin to streptavidin. For this purpose, recoverin solutions were injected into a flow cell without immobilized liposomes. Values of R_{eq} were obtained as above and subtracted from R_{eq} values acquired with immobilized liposomes to yield ΔR_{eq}. Kinetic data were evaluated from fitting the association and dissociation phase of sensorgrams to double exponentials. The association phase was described with the time constants k_{s1}, k_{s2}: $R(t) = R_{eq1}(1 - e^{-k_{s1}t}) + R_{eq2}(1 - e^{-k_{s2}t})$; the dissociation phase was described with the time constants k_{d1}, k_{d2}:

$$R(t) = R_0\left[\frac{R_1}{R_0}e^{-k_{d1}t} + \left(1 - \frac{R_1}{R_0}\right)e^{-k_{d2}t}\right]$$

Fits were applied to the entire association phase starting immediately after completion of buffer exchange (4 s after injection) and to the entire dissociation phase starting also 4 s after the end of sample injection. Nonlinear curve fitting to sensorgrams was done with the BIAevaluation 2.1 software, while all other data processing was performed with SIGMA Plot for Windows 2.1 (Jandel).

Ca^{2+} Buffer. Ca^{2+} buffers were prepared as described by Tsien and Pozzan (*35*) by addition of stock solutions of K_2H_2-EGTA and $K_2CaEGTA$ to a final concentration of 2 mM total EGTA. Measurements at Ca^{2+} saturation were performed with 2 mM $CaCl_2$ and no EGTA added. Free [Ca^{2+}] was calculated with the CHELATOR buffer program (Schoenmakers, Nijmegen, Netherlands) using the constants of Martell and Smith (*36*). Buffer solutions were checked spectrophotometrically with dibromo-BAPTA as indicator by measuring Ca^{2+}-sensitive absorption changes at 264 nm. A calibration curve was calculated using a Ca^{2+} dissociation constant of 3.47 μM for dibromo-BAPTA (a K_D of 1.58 μM was taken from ref *37* and extrapolated to the conditions of our assay system, T = 25 °C and pH 7.1, according to ref *37* and the CHELATOR buffer program).

RESULTS

The Ca^{2+}−myristoyl switch of recoverin can be monitored in real time by surface plasmon resonance spectroscopy using two different configurations, with recoverin as analyte and liposomes as ligand or vice versa. Either acylated or nonacylated recoverin was immobilized on the sensor chip dextran surface through thiol coupling. Alternatively, recoverin was coupled through free amino groups without a significant difference in coupling yields or membrane binding characteristics. Large unilamellar vesicles, that have been applied in the analyte phase, bound to recoverin in a Ca^{2+}-dependent fashion (Figure 1A). This can be seen in Figure 1A as an increase in resonance units, when 2 mM $CaCl_2$ was present. Sensorgrams with an excess of EGTA in the running buffer showed a negative change in resonance units due to a buffer-induced change in bulk refractive index (Figure 1 A, trace with EGTA). The complex formation of recoverin with liposomes was reversible. Flushing the flow cell with running buffer containing no liposomes (open bar in Figure 1A) led to a decrease in resonance units, indicating dissociation of liposomes from immobilized recoverin. Complete dissociation was achieved by a pulse of 1% Tween in running buffer (hatched bar) without $CaCl_2$. Besides Ca^{2+},

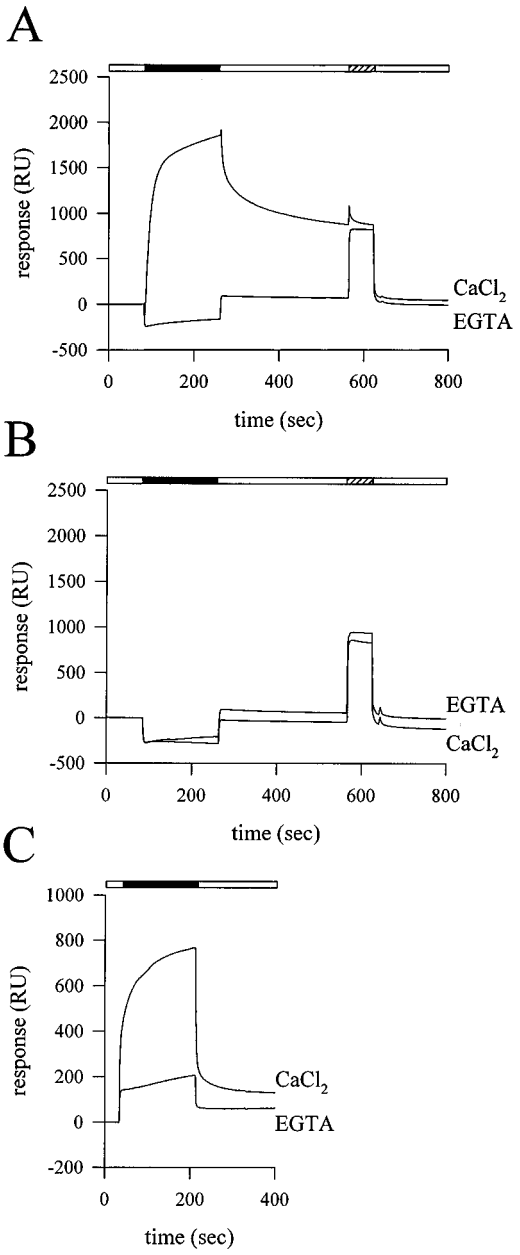

FIGURE 1: Ca^{2+}−myristoyl switch of recoverin monitored by SPR spectroscopy. Native acylated (A) or recombinant nonacylated recoverin (B) was immobilized on a biosensor chip via thiol coupling. Sensorgrams were recorded with liposomes as analyte in running buffer (horizontal filled bar) in the presence of 2 mM $CaCl_2$ or 2 mM EGTA. Open bars represent flow of running buffer. Injection of 1% Tween (hatched bar) resulted in the complete dissociation of recoverin and liposomes. (C) Sensorgrams with reversed geometric configuration. Biotin-labeled liposomes were immobilized on a streptavidin-coated sensor chip surface. The displayed sensorgram shows the Ca^{2+}-dependent binding of 10 μM native recoverin (horizontal filled bar) as analyte. No binding was observed without Ca^{2+} in the running buffer.

the interaction of recoverin and liposomes also required the presence of the myristoyl group in recoverin. Phospholipid vesicles did not bind to immobilized nonmyristoylated recoverin (Figure 1B). This Ca^{2+}-dependent binding of recoverin to membranes can also be monitored with a reversed geometry. Phospholipid vesicles containing biotinylated phosphatidylethanolamine were immobilized via biotin−streptavidin coupling on a streptavidin-coated sensor chip. Immobilization levels between 5800 and 8000 RU were obtained. The base line varied within less than 5 RU over 12 h (flow rate 10 μL/min of running buffer). Occasionally, within the first hour after immobilization, an increase of the signal by up to 60 RU was observed. Thus, the immobilization of liposomes was stable for the entire recording time of 10 h. Native recoverin in the analyte phase bound to immobilized liposomes only in the presence of Ca^{2+} (Figure 1C). Only a small increase in resonance units was observed in the presence of EGTA. This change was also due to a buffer-induced change in the bulk refractive index. The change seen in Figure 1C was positive and not negative as in Figure 1A,B, because the buffer composition was slightly different. We experienced that small differences in buffer composition can cause these differences in bulk refractive index changes. Complex formation of recoverin with liposomes was reversible in both geometric configurations (Figure 1A,C). Maximal amplitudes in sensorgrams with liposomes as analyte were generally larger than in sensorgrams with recoverin as analyte (up to 8000 RU compared to maximal 2000 RU). This difference is mainly attributed to the large mass of a single liposome when compared to one recoverin molecule. Another difference was evident in the dissociation phase. Recoverin as analyte dissociated faster from the immobilized liposomes (Figure 1C) than the liposomes from immobilized recoverin (Figure 1A).

Recoverin binds two Ca^{2+} ions with apparent dissociation constants of 0.11 μM and 6.9 μM (*13*). Therefore, we expected an EC_{50} of the Ca^{2+}−myristoyl switch between 0.1 and 10 μM Ca^{2+}. Surprisingly, we did not observe any significant binding of recoverin to immobilized liposomes up to 100 μM Ca^{2+}. Instead, binding of recoverin was only observed at millimolar [Ca^{2+}] (Figure 1). This binding was strongly influenced by $MgCl_2$. We added 2, 10, and 20 mM $MgCl_2$ to the running buffer and observed a shift in the Ca^{2+} sensitivity to lower [Ca^{2+}] (Figure 2A−C). At 20 mM $MgCl_2$, we achieved saturation of the association curves at 100 μM Ca^{2+} (Figure 2C). Thus, we needed $MgCl_2$ to titrate the Ca^{2+} sensitivity of the recoverin/liposome interaction in a reasonable range of [Ca^{2+}]. The need for Mg^{2+} ions in our Ca^{2+} titration experiments probably reflects a property of the dextran layer on the sensor chip surface, where free carboxy groups have exposed binding sites for divalent cations. In addition, phospholipids bind divalent cations.

In order to determine the half-maximal [Ca^{2+}] of the switch, sensorgrams of interactions between recoverin and liposomes were recorded with both geometric configurations (see above) at different [Ca^{2+}]. Figure 3 shows sensorgrams with either liposomes (Figure 3A) or 30 μM recoverin (Figure 3C) as analyte. Resonance units at equilibrium, R_{eq}, when the net binding rate is zero, were determined from fitting the data as described under Materials and Methods, normalized for each independent experiment to the value obtained at 1 mM Ca^{2+}, pooled and plotted as a function of the free [Ca^{2+}] (Figure 3B). The binding of liposomes to immobilized recoverin was half-maximal at 7.7 μM Ca^{2+} (Figure 3B).

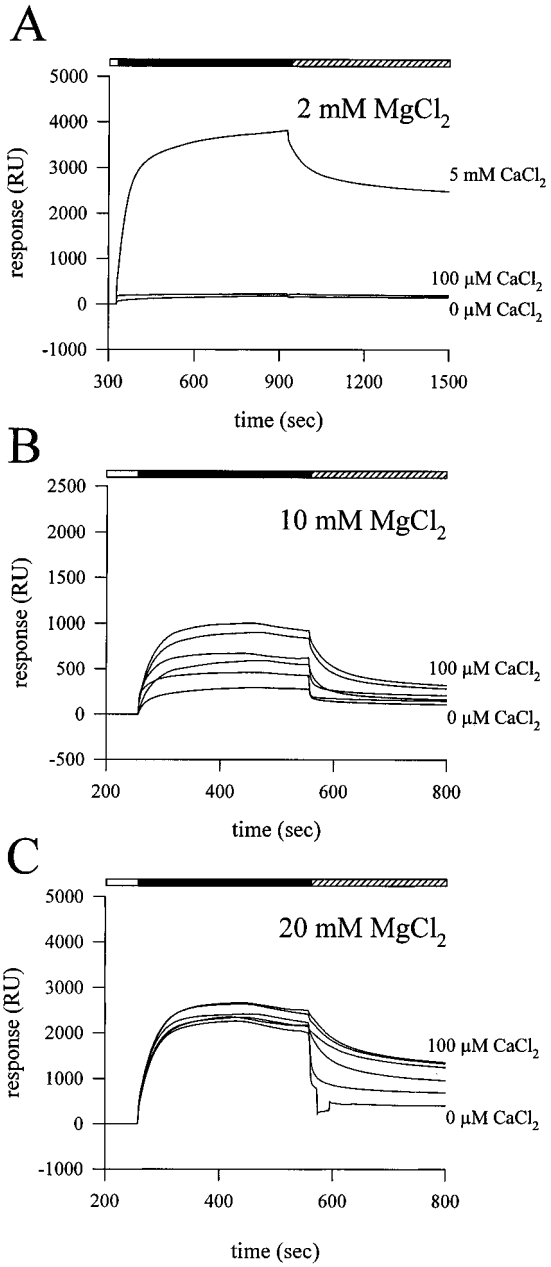

FIGURE 2: Influence of Mg^{2+} on Ca^{2+}-dependent interaction of liposomes with immobilized recoverin. Recoverin was immobilized as in Figure 1, and sensorgrams in (A)−(C) were recorded with liposomes (0.2 mM phosphate) as analyte (horizontal filled bars) at different concentrations of $MgCl_2$ and $CaCl_2$. The corresponding conditions were (A) 2 mM $MgCl_2$ and 0, 100, and 5000 μM $CaCl_2$; (B) 10 mM $MgCl_2$ and 0, 5, 10, 20, 50, and 100 μM $CaCl_2$; and (C) 20 mM $MgCl_2$ and 0, 5, 10, 20, 50, and 100 μM $CaCl_2$. Please note that concentrations of indicated $CaCl_2$ mean added $CaCl_2$. For instance, sensorgrams at 0 μM added $CaCl_2$ were recorded at micromolar [Ca^{2+}] that is present in double-distilled water. Dissociation started when Ca^{2+} but no liposomes was in the running buffer (hatched bars), whereas running buffer before application of liposomes contained no $CaCl_2$ (open bars).

In Figure 3C, we recorded sensorgrams with immobilized liposomes and recoverin as analyte. Recoverin also adsorbed to the streptavidin on the sensor chip surface, giving signals that were smaller than those indicating binding to liposomes. Therefore, values were corrected for nonspecific binding of recoverin to streptavidin. Since we have no possibility to

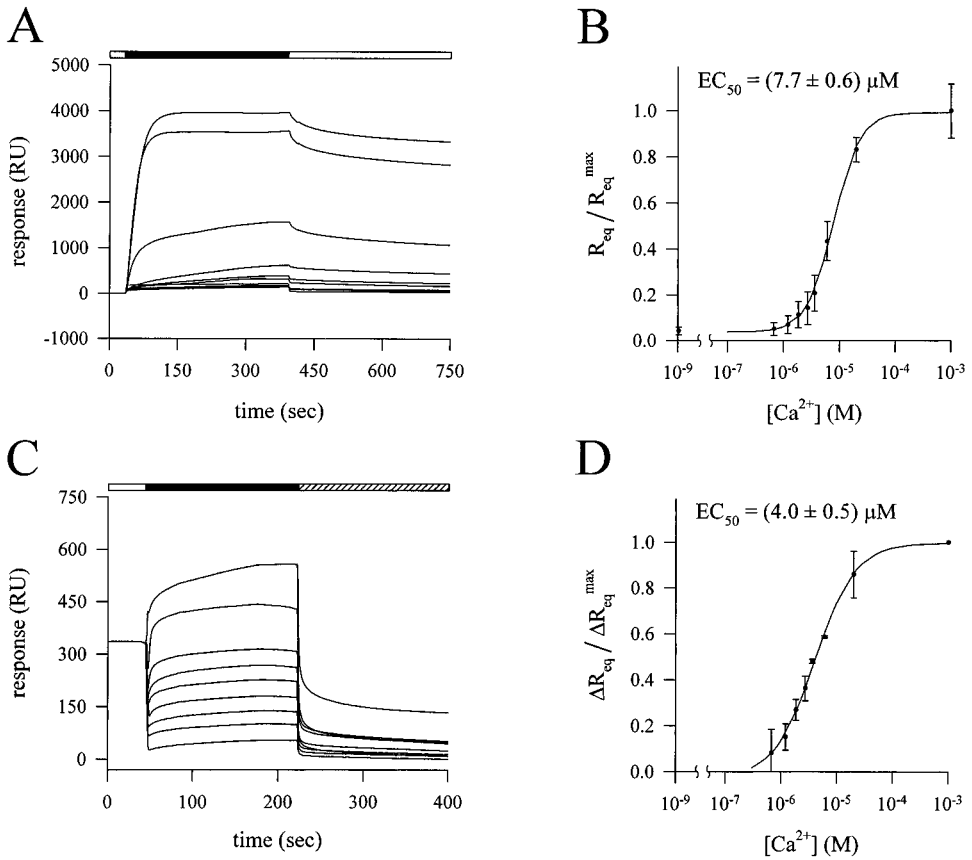

FIGURE 3: Ca^{2+} titration of recoverin−liposome interaction. Running buffer contained 2 mM EGTA and 20 mM $MgCl_2$ (open bars). The binding process was studied by two different geometric configurations with (A) liposomes (0.2 mM phosphate) or (C) 30 μM recoverin as analyte in sample buffer (horizontal filled bars). The sample buffer contained 20 mM $MgCl_2$ and 2 mM EGTA/Ca^{2+} buffer with free [Ca^{2+}] at 1 nM, 679 nM, 1.21 μM, 1.85 μM, 2.7 μM, 3.59 μM, 6.0 μM, 19.8 μM, and 1 mM. The hatched bar in (C) indicates flow of sample buffer without analyte. Sensorgrams were fitted as described under Materials and Methods. Resulting R_{eq} and ΔR_{eq} values were normalized to the values obtained at 1 mM [Ca^{2+}] (i.e., R_{eq}^{max} and ΔR_{eq}^{max}) and plotted as a function of the free [Ca^{2+}] in (B) and (D), respectively. The Ca^{2+}-dependent interaction was half-maximal at 7.7 μM (A, B) and 4.0 μM (C, D). The ΔR_{eq} values in (D) were obtained after subtraction of nonspecific binding of recoverin to streptavidin. (A) and (C) show individual representative experiments. Data points in panel (B) represent mean values of four data sets from two independent experiments. Data points in panel (D) denote mean values of two independent experiments. Error bars denote the standard deviation.

determine binding of recoverin to streptavidin in the presence of liposomes, we subtracted the streptavidin-binding signal in the absence of liposomes from the specific binding signal in the presence of liposomes, yielding ΔR_{eq} values (see Materials and Methods). It is plausible that undesirable binding of recoverin to streptavidin in the presence of liposomes is smaller than in their absence. Thus, corrected ΔR_{eq} values might underestimate true values. The Ca^{2+}-dependent binding of myristoylated recoverin to immobilized liposomes was half-maximal at 4.0 μM Ca^{2+} (Figure 3D). This EC_{50} value was similar to the EC_{50} value of 7.7 μM Ca^{2+} determined with a geometric configuration, when the nonspecific binding of recoverin to streptavidin was absent (Figure 3A,B). Therefore, nonspecific binding does not compromise the determination of the Ca^{2+}-dependent binding.

What is the affinity for binding of recoverin in its Ca^{2+} form to membranes? The affinity was determined by recording sensorgrams at increasing recoverin concentrations ranging from 3 to 100 μM at saturating free [Ca^{2+}] (Figure 4A). However, binding of recoverin did not saturate over this physiological range of recoverin concentrations (*38*). At larger concentrations, recoverin aggregates (*39*) which precludes reproducible SPR experiments. ΔR_{eq} values were normalized for each individual experiment with an ΔR_{eq}^{max} value obtained from a Scatchard plot (data not shown). Values for K_D determined from Scatchard plots of individual experiments ranged from 120 to 240 μM with a mean of 160 μM. Normalized responses were plotted as a function of the recoverin concentration and were fitted to a simple binding isotherm with an apparent K_D of 160 μM (Figure 4B). A Scatchard plot of the pooled data gave a similar K_D value (Figure 4C; K_D = 140 μM). The amplitude of the specific binding signal was correlated to the amount of immobilized liposomes. The maximal specific binding response to immobilized liposomes obtained with 100 μM recoverin ranged between 600 and 1300 RU, corresponding to 0.6−1.3 ng/mm^2.

ROS liposomes were immobilized via biotin−streptavidin coupling similar to the coupling of phospholipid liposomes. Sensorgrams were recorded at increasing recoverin concentrations, and data were evaluated in the same manner as for the interaction of recoverin with phospholipid liposomes (Figure 5A−C). We performed five independent immobilization experiments using five different ROS liposome preparations. Each preparation was titrated with 8−10 different recoverin concentrations. Resulting K_D values in individual experiments were 2, 27, 31, 74, and 181 μM. These data sets showed a larger scattering than the data

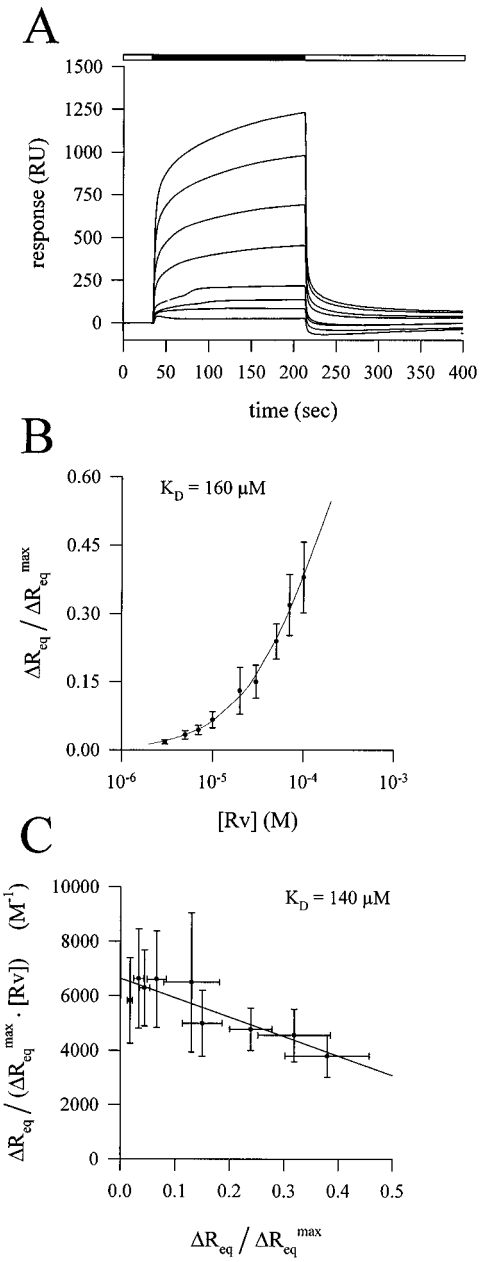

FIGURE 4: Affinity of native recoverin for phospholipid membranes at 2 mM free Ca^{2+}. (A) Sensorgrams were recorded with varying concentrations of native recoverin (3−100 μM) in a buffer with 20 mM $MgCl_2$ and 2 mM $CaCl_2$ (horizontal filled bar). Open bars represent running buffer with 2 mM EGTA. (B) Plot of normalized ΔR_{eq} values against recoverin concentration [Rv]. Data points represent mean values of five data sets from three independent experiments. The K_D was 160 μM. (C) Scatchard plot of the data sets shown in (B). The K_D was 140 μM.

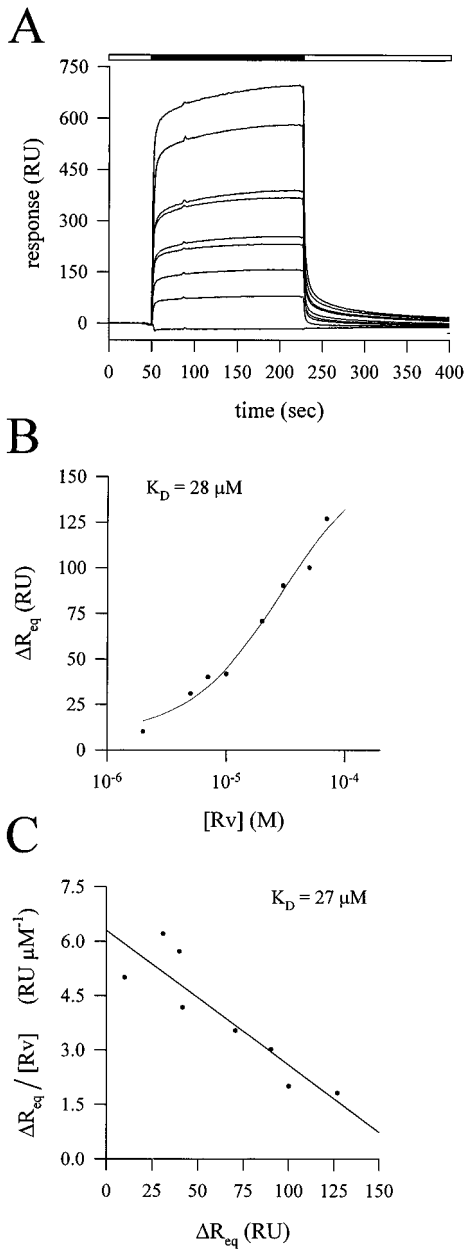

FIGURE 5: Affinity of native recoverin for ROS membranes at 2 mM free Ca^{2+}. (A) Sensorgrams were recorded with varying concentrations of native recoverin (2−70 μM) in a buffer with 20 mM $MgCl_2$ and 2 mM $CaCl_2$ (horizontal filled bar). Open bars represent running buffer with 2 mM EGTA. (B) Plot of ΔR_{eq} values against recoverin concentration [Rv] using the data of the sensorgrams in (A). (C) Scatchard plot of the data set shown in (B). The K_D was 27 μM.

obtained with pure phospholipid liposomes. ROS liposomes contained membrane proteins and cytoskeletal elements which probably caused more heterogeneity on the surface of the biosensor chip than immobilized phospholipid liposomes. However, in most cases the affinity of recoverin for ROS membranes was higher. Experiments with extracted native ROS lipids failed, because the base line was very unstable and showed a large drift of 6000 RU (equivalent to a loss of more than two-thirds of immobilized lipid) within 24 h.

Kinetics of recoverin binding to immobilized liposomes were very rapid. The association and dissociation phases could not be described by a simple binding model (A + B ↔ AB). Therefore, the association phase of sensorgrams was fitted by a double exponential, yielding time constants k_{s1} and k_{s2}. Similarly, the dissociation phase of sensorgrams was fitted by double exponentials, yielding time constants termed k_{d1} and k_{d2}. In both cases, the contribution of fast and slow components to the total response was approximately equal. Fast time constants were of the order of 0.1 s^{-1}; slow components were of the order of 0.01 s^{-1}. No difference in the kinetics was apparent when we compared the binding of recoverin to ROS liposomes with its binding to phospholipid liposomes (Figures 4 and 5). Reported time constants do not represent true chemical rate constants. Probably, the apparent kinetics of the binding signals were dominated by

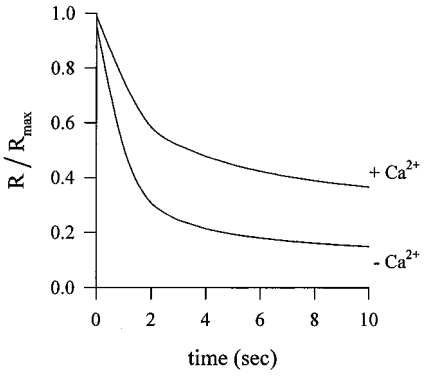

FIGURE 6: Dissociation of recoverin from immobilized liposomes at 1 mM (+ Ca^{2+}) and subnanomolar (−Ca^{2+}) free [Ca^{2+}]. The first 10 s of the dissociation phase of two sensorgrams obtained under identical buffer conditions in the association phase was superimposed. This interval was chosen to highlight the different kinetics.

transport of recoverin to the immobilized liposomes, e.g., diffusion through the aqueous nonstirred boundary layer *(40, 41)*. The time constants, however, do allow the determination of relative differences in kinetics. For example, how much different is the dissociation rate of the recoverin−membrane complex at high [Ca^{2+}] from the rate at low [Ca^{2+}]? In the range from subnanomolar to micromolar [Ca^{2+}], k_s values increased 2−3-fold, while k_d values decreased to the same degree. When an injection of recoverin at 1 mM Ca^{2+} was followed by buffer containing subnanomolar [Ca^{2+}], 80% of bound recoverin was released from the membrane within 3 s, whereas dissociation into buffer containing millimolar [Ca^{2+}] occurred approximately 3-fold slower (Figure 6). The Ca^{2+}-dependent differences in k_s and k_d values point to an approximately 10-fold difference in the affinity of recoverin for membranes.

DISCUSSION

Surface plasmon resonance spectroscopy can be successfully used to monitor a Ca^{2+}−myristoyl switch of a Ca^{2+}-sensor like recoverin. The experimental approach allows the determination of affinity constants and kinetic parameters. At saturating [Ca^{2+}], the affinity of recoverin to phospholipids was rather low with a K_D of 140−160 μM [$K_A = (6-7) \times 10^3\ M^{-1}$] (Figure 4). This affinity was almost identical to the association constant of myristoylated model peptides with lipids ($K_A = 10^4\ M^{-1}$, ref *42*), but 1000-fold lower than the affinity of intact Src protein for phospholipids ($K_A = 10^7\ M^{-1}$, ref *43*). Src has a cluster of basic residues (G_2−R_{15}, net charge = +5) following the myristoyl group. Electrostatic interactions of this cluster with acidic phospholipids contribute significantly to the high binding affinity (*43*). The corresponding region in bovine recoverin (G_2−R_{16}; ref *44*) contains two lysines and three glutamate residues and has a completely different charge distribution (net charge = −1). Therefore, the hydrophobic interaction by the myristoyl group seems to be more important than electrostatic interactions in the Ca^{2+} switch of recoverin. This is in agreement with the observation in Figure 1 that nonmyristoylated recoverin does not associate with phospholipids irrespective of the free [Ca^{2+}]. These findings make it also quite unlikely that the only apparent cluster of basic residues in recoverin located in the carboxy terminus (K_{192}−L_{202}, six lysine and two glutamate residues) contributes significantly to the membrane association of recoverin which is also consistent with the finding of Dizhoor et al. (1993) that recoverin truncated at the carboxy terminus can bind to membranes (*7*). The affinity of recoverin binding to ROS liposomes appeared higher in most experiments, but the large scattering of the data does not allow a definitive conclusion about the exact K_D value. The immobilization of ROS liposomes containing integral membrane proteins and cytoskeletal elements resulted in heterogeneous surfaces on dextran-coated sensor chips.

The same experimental configuration (immobilized phospholipids and recoverin as analyte) has been used to determine the half-maximal [Ca^{2+}] of the switch. We cannot entirely exclude that the high concentration of $MgCl_2$, which is necessary in our assay system, interferes with the Ca^{2+} binding of recoverin. One could argue that Mg^{2+} at these high concentrations competes with Ca^{2+} for the binding sites on recoverin. Any competition of Mg^{2+} would then increase the EC_{50} of the Ca^{2+} switch. However, as shown in Figure 2, increasing [$MgCl_2$] shifted the dose−response curve to lower free [Ca^{2+}]. The main effect of this high concentration of Mg^{2+} is to screen negatively charged groups in the dextran layer and on the membrane surface. An EC_{50} value for [Ca^{2+}] of 4.0 μM is similar to the EC_{50} of 2.1 μM determined by Zozulya and Stryer (*6*) with tritiated myristoylated recoverin in an equilibrium centrifugation assay. These values also agree well with the half-maximal [Ca^{2+}] of 1.5−3 μM needed to inhibit rhodopsin kinase by myristoylated recoverin (*21, 24*). In order to reconcile these relatively high [Ca^{2+}] with that prevailing in a photoreceptor at rest, authors extrapolate their *in vitro* data to concentrations of binding partners *in vivo* (*6, 21*). However, we conclude that the recording of a Ca^{2+}−myristoyl switch in the biosensor flow chamber particularly with an immobilized phospholipid bilayer is a good approximation of the situation on a disk surface for the following reasons. First, in the flow chamber, liposomes are immobilized to the surface of the sensor chip like phospholipid bilayers held together by a network of cytoskeletal elements in a living cell. Immobilized liposomes and recoverin do not form a dilute mixture like they would in a reaction tube or in a cuvette. Second, when recoverin was applied as analyte in the running buffer, we varied the concentration of recoverin in the physiological range (3−100 μM). Our experiments were not limited by an insufficient amount of recoverin in the flow cell.

We interpret our data in Figure 3D as that most of the recoverin pool is not associated with liposomes at 500 nM free [Ca^{2+}]. However, the amount of recoverin associated with ROS membranes may be higher due to the apparent higher affinity of recoverin to ROS liposomes and thus may be sufficient to form a stabilized Ca^{2+}−recoverin−rhodopsin kinase complex (*25*). On the other hand, most of the recoverin in the rod seems to be soluble at levels of [Ca^{2+}] in the dark-adapted state and may serve other functions in the Ca^{2+}-mediated feedback loops which are part of the molecular basis of light adaptation (*38, 45, 46*).

ACKNOWLEDGMENT

We thank Mrs. D. Höppner-Heitmann for excellent technical assistance and Drs. E. Eismann, U. B. Kaupp, and R. Seifert for critical comments on the manuscript.

REFERENCES

1. Towler, D. A., Gordon, J. I., Adams, S. P., and Glaser, L. (1988) *Annu. Rev. Biochem. 57*, 69−99.
2. McLaughlin, S., and Aderem, A. (1995) *Trends Biochem. Sci. 20*, 272−276.
3. Franco, M., Chardin, P., Chabre, M., and Paris, S. (1996) *J. Biol. Chem. 271*, 1573−1578.
4. Boman, A. L., and Kahn, R. A. (1995) *Trends Biochem. Sci. 20*, 147−150.
5. Thelen, M., Rosen, A., Nairn, A. C., and Aderem, A. (1991) *Nature 351*, 320−322.
6. Zozulya, S., and Stryer, L. (1992) *Proc. Natl. Acad. Sci. U.S.A. 89*, 11569−11573.
7. Dizhoor, A. M., Chen, C.-K., Olshevskaya, E., Sinelnikova, V. V., Phillipov, P., and Hurley, J. B. (1993) *Science 259*, 829−832.
8. Ladant, D. (1995) *J. Biol. Chem. 270*, 3179−3185.
9. Faurobert, E., Chen, C.-K., Hurley, J. B., and Teng, D. H.-F. (1996) *J. Biol. Chem. 271*, 10256−10262.
10. Kobayashi, M., Takamatsu, K., Saitoh, S., and Noguchi, T. (1993) *J. Biol. Chem. 268*, 18898−18904.
11. Ames, J. B., Tanaka, T., Stryer, L., and Ikura, M. (1994) *Biochemistry 33*, 10743−10753.
12. Ames, J. B., Tanaka, T., Ikura, M., and Stryer, L. (1995) *J. Biol. Chem. 270*, 30909−30913.
13. Ames, J. B., Porumb, T., Tanaka, T., Ikura, M., and Stryer, L. (1995) *J. Biol. Chem. 270*, 4526−4533.
14. Tanaka, T., Ames, J. B., Harvey, T. S., Stryer, L., and Ikura, M. (1995) *Nature 376*, 444−447.
15. Hughes, R. E., Brzovic, P. S., Klevit, R. E., and Hurley, J. B. (1995) *Biochemistry 34*, 11410−11416.
16. Ames, J. B., Tanaka, T., Stryer, L., and Ikura, M. (1996) *Curr. Opin. Struct. Biol. 6*, 432−438.
17. Kawamura, S. (1993) *Nature 362*, 855−857.
18. Kawamura, S., Hisatomi, O., Kayada, S., Tokunaga, F., and Kuo, C.-H. (1993) *J. Biol. Chem. 268*, 14579−14582.
19. Gray-Keller, M. P., Polans, A. S., Palczewski, K., and Detwiler, P. B. (1993) *Neuron 10*, 523−531.
20. Gorodovikova, E. N., Senin, I. I., and Philippov, P. P. (1994) *FEBS Lett. 353*, 171−172.
21. Klenchin, V. A., Calvert, P. D., and Bownds, M. D. (1995) *J. Biol. Chem. 270*, 16147−16152.
22. Kawamura, S., Cox, J. A., and Nef, P. (1994) *Biochem. Biophys. Res. Commun. 203*, 121−127.
23. Calvert, P. D., Klenchin, V. A., and Bownds, M. D. (1995) *J. Biol. Chem. 270*, 24127−24129.
24. Senin, I. I., Zargarov, A. A., Alekseev, A. M., Gorodovikova, E. N., Lipkin, V. M., and Philippov, P. P. (1995) *FEBS Lett. 376*, 87−90.
25. Sanada, K., Shimizu, F., Kameyama, K., Haga, K., Haga, T., and Fukada, Y. (1996) *FEBS Lett. 384*, 227−230.
26. Szabo, A., Stolz, L., and Granzow, R. (1995) *Curr. Opin. Struct. Biol. 5*, 699−705.
27. Jönsson, U., Fägerstam, L., Ivarsson, B., Johnsson, B., Karlsson, R., Lundh, K., Löfås, S., Persson, B., Roos, H., Rönnberg, I., Sjölander, S., Sternberg, E., Ståhlberg, R., Urbaniczky, C., Östlin, H., and Malmqvist, M. (1991) *BioFeature 11*, 620−627.
28. O'Shannessy, D. J., Brigham-Burke, M., Soneson, K. K., Hensley, P., and Brooks, I. (1994) *Methods Enzymol. 240*, 323−349.
29. Lambrecht, H.-G., and Koch, K.-W. (1991) *EMBO J. 10*, 793−798.
30. Polans, A. S., Buczylko, J., Crabb, J., and Palczewski, K. (1991) *J. Cell Biol. 112*, 981−989.
31. Frins, S., Bönigk, W., Müller, F., Kellner, R., and Koch, K.-W. (1996) *J. Biol. Chem. 271*, 8022−8027.
32. Anderson, R. E., and Maude, M. B. (1970) *Biochemistry 9*, 3624−3628.
33. Bartlett, G. R. (1959) *J. Biol. Chem. 234*, 466.
34. Masson, L., Mazza, A., and Brousseau, R. (1994) *Anal. Biochem. 218*, 405−412.
35. Tsien, R., and Pozzan, T. (1989) *Methods Enzymol. 172*, 230−262.
36. Martell, A. E., and Smith, R. M. (1974) *Critical Stability Constants*, Plenum Press, New York.
37. Harrison, S. M., and Bers, D. M. (1987) *Biochim. Biophys. Acta* 925, 133−143.
38. Koch, K.-W. (1994) *Rev. Physiol. Biochem. Pharmacol. 125*, 149−192.
39. Kataoka, M., Mihara, K., and Tokunaga, F. (1993) *J. Biochem. 114*, 535−540.
40. Schuck, P. (1996) *Biophys. J. 70*, 1230−1249.
41. Schuck, P., and Minton, A. P. (1996) *Anal. Biochem. 240*, 262−272.
42. Peitzsch, R. M., and McLaughlin, S. (1993) *Biochemistry 32*, 10436−10443.
43. Buser, C. A., Sigal, C. T., Resh, M. D., and McLaughlin, S. (1994) *Biochemistry 33*, 13093−13101.
44. Dizhoor, A. M., Ray, S., Kumar, S., Niemi, G., Spencer, M., Brolley, D., Walsh, K. A., Philipov, P. P., Hurley, J. B., and Stryer, L. (1991) *Science 251*, 915−918.
45. Koutalos, Y., and Yau, K.-W. (1996) *Trends Neurosci. 19*, 73−81.
46. Detwiler, P. B., and Gray-Keller, M. P. (1996) *Curr. Opin. Neurobiol. 6*, 440−444.

BI970938D